

# Low Complexity Decoding of BICM STBC

Enis Akay and Ender Ayanoglu

Center for Pervasive Communications and Computing  
Department of Electrical Engineering and Computer Science  
The Henry Samueli School of Engineering  
University of California, Irvine  
Irvine, California 92697-2625  
Email: eakay@uci.edu ayanoglu@uci.edu

**Abstract**—It was shown earlier that the combination of bit interleaved coded modulation (BICM) with space time block codes (STBC) for OFDM systems leads to the maximum diversity order in space and frequency. In this paper we present low complexity decoding of BICM-STBC systems. First, the maximum likelihood (ML) bit metric calculations are simplified from a distance on the complex plane to a distance on the real line. Furthermore, we present log-likelihood-ratio (LLR) approximations to maximum likelihood (ML) decoding metrics to achieve easier to implement soft decision bit metrics with the same high performance. The LLR bit metrics are specifically calculated for  $M$ -ary QAM signal constellations used in IEEE 802.11a/g networks. Simulation results also show that while achieving a substantial improvement in decoder complexity, the proposed bit metrics achieve the same high performance.

## I. INTRODUCTION

In order to combat severe conditions of wireless channels, different diversity techniques (such as temporal, frequency, spatial and code diversity) have been developed in the literature. Zehavi showed that code diversity could be improved by bit-wise interleaving [1]. Using an appropriate soft-decision bit metric at a Viterbi decoder, Zehavi achieved a code diversity equal to the smallest number of distinct bits, rather than channel symbols, along any error event. This difference between bit-wise interleaving and symbol interleaving results in improved performance for BICM over a fading channel when compared to Ungerboeck's trellis coded modulation (TCM, [2]) [1]. Following Zehavi's work, Caire *et al.* [3] presented the theory behind BICM. Their work provided tools to evaluate the performance of BICM with tight error probability bounds and design guidelines.

In recent years using multiple antennas has become an important tool to exploit the diversity in spatial domain. Space time trellis codes (STTC) [4], and space time block codes [5], [6] were developed to achieve the maximum space diversity. In this approach the channel is assumed to be frequency nonselective. However, when there is frequency selectivity in the channel, the design of appropriate space-time codes becomes a more complicated problem due to the existence of intersymbol interference (ISI). On the other hand, frequency selective channels offer additional frequency diversity [7], [8], and carefully designed systems can exploit this property. OFDM is known to combat ISI very effectively, and therefore

can simplify the code design problem for frequency selective channels. It was shown in [9] that BICM with OFDM can achieve the maximum frequency diversity. Using multiple antennas and by applying STBC to BICM OFDM systems, one can achieve the maximum diversity in frequency and space [10].

It was shown in [11], [12], and [13] that the decoding complexity of BICM can be lowered substantially without any performance degradation. In this paper we show that low complexity decoding of BICM-STBC systems can be easily achieved by using the ideas in [11] and [13] in combination with the fact that STBC are capable of separate decoding. For square  $M$ -ary QAM constellations, we will show that the bit metric calculations can be simplified from a distance on the complex plane over  $M/2$  constellation points to a distance on the real line over  $\sqrt{M}/2$  points. In addition, for QAM constellations of 802.11a/g, we present LLR bit metrics with the same high performance.

Sections II and III present brief overviews of BICM and STBC, respectively. The bit metrics of BICM-STBC systems, and their low complexity counterparts are introduced in Section IV. Simulation results showing that the low complexity bit metrics achieve the same high performance are presented in Section V. Finally, we conclude our paper with a brief conclusion in Section VI.

## II. BIT-INTERLEAVED CODED MODULATION (BICM)

BICM can be obtained by using a bit interleaver,  $\pi$ , between an encoder for a binary code  $\mathcal{C}$  and a memoryless modulator over a signal set  $\chi \subseteq \mathbb{C}$  of size  $|\chi| = M = 2^m$  with a binary labeling map  $\mu : \{0, 1\}^m \rightarrow \chi$ . Gray encoding is used to map the bits onto symbols. During transmission, the code sequence  $\underline{c}$  is interleaved by  $\pi$ , and then mapped onto the signal sequence  $\underline{x} \in \chi$ . The signal sequence  $\underline{x}$  is then transmitted over the channel.

The bit interleaver can be modeled as  $\pi : k' \rightarrow (k, i)$  where  $k'$  denotes the original ordering of the coded bits  $c_{k'}$ ,  $k$  denotes the time ordering of the signals  $x_k$  transmitted, and  $i$  indicates the position of the bit  $c_{k'}$  in the symbol  $x_k$ .

Let  $\chi_b^i$  denote the subset of all signals  $x \in \chi$  whose label has the value  $b \in \{0, 1\}$  in position  $i$ . Then, the ML bit metrics

can be given by [1], [3]

$$\lambda^i(y_k, c_{k'}) = \min_{x \in \chi_{c_{k'}}^i} \|y_k - \rho x\|^2 \quad (1)$$

where  $\rho$  denotes the Rayleigh coefficient and  $\|(\cdot)\|^2$  represents the squared Euclidean norm of  $(\cdot)$ .

The ML decoder at the receiver can make decisions according to the rule

$$\hat{c} = \arg \min_{c \in C} \sum_{k'} \lambda^i(y_k, c_{k'}). \quad (2)$$

### III. SPACE TIME BLOCK CODES (STBC)

Complex orthogonal space time block codes are considered in this paper. For  $N$  transmit antennas,  $S/T$  rate STBC is defined as the complex orthogonal block code which transmits  $S$  symbols over  $T$  time slots. The code generator matrix  $G_{STN}$  is a  $T \times N$  matrix and satisfies

$$G_{STN}^H G_{STN} = \gamma(|x_1|^2 + |x_2|^2 + \dots + |x_S|^2) I_N \quad (3)$$

where  $\gamma$  is a positive constant and  $\{x_i\}_{i=1}^S$  are the complex symbols transmitted in one STBC codeword.

Space time block codes allow separate decoding at the receiver for each symbol  $x_s$  transmitted within the code  $C = G_{STN}(x_1, x_2, \dots, x_S)$ . The metric to be minimized in order to decode each symbol can be written as [6]

$$|y - x|^2 + \beta |x|^2 \quad (4)$$

where the minimization is taken over  $x$  within the constellation set that the symbols are modulated onto. The numbers  $y \in \mathbb{C}$  and  $\beta \in \mathbb{R}$ , and they are calculated depending on the symbol to be detected and STBC that is used. For example, for the Alamouti code

$$\beta = -1 + \sum_{m=1}^M \sum_{n=1}^N |\alpha_{n,m}|^2$$

$$y = \sum_{m=1}^M (r_{1,m} \alpha_{1,m}^* + r_{2,m}^* \alpha_{2,m}) \text{ to detect } x_1 \quad (5)$$

$$y = \sum_{m=1}^M (r_{1,m} \alpha_{2,m}^* - r_{2,m}^* \alpha_{1,m}) \text{ to detect } x_2 \quad (6)$$

where  $r_{t,m}$ ,  $t = 1, 2, \dots, T$ ,  $m = 1, 2, \dots, M$  is

$$r_{t,m} = \sum_{n=1}^N c_{t,n} \alpha_{n,m} + n_{t,m} \quad (7)$$

with  $c_{t,n}$  denoting the  $(t, n)^{th}$  element of the space time code  $C$  and  $\alpha_{n,m}$  is the path gain from the  $n$ th transmit antenna to the  $m$ th receive antenna, and  $n_{t,m}$  is the AWGN.

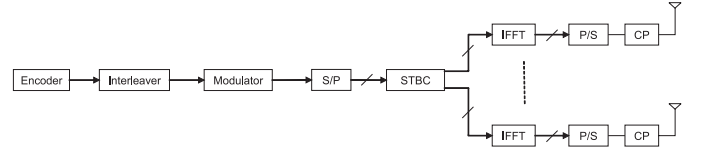


Fig. 1. Block diagram of transmission with BICM STBC for OFDM systems

### IV. BICM-STBC BIT METRICS

The BICM-STBC system is implemented by concatenating BICM and STBC. The bits are first encoded using a convolutional encoder and then interleaved. The interleaved bits are then modulated onto symbols using a signal map. The symbols are then coded in space and time using an appropriate STBC.

BICM-OFDM provides maximum frequency diversity [9]. If OFDM is used with BICM-STBC, then after the modulator the symbols are switched from serial to parallel with the number of subcarriers used for one OFDM symbol. Note that, the bit metrics shown here can be used for any BICM-STBC system regardless of whether OFDM is being used or not. The reason that the symbols are grouped into vectors, and STBC is applied on the vectors is to achieve the maximum frequency and space diversity with BICM-STBC-OFDM [10].

Assume that the coded bit  $c_{k'}$  is mapped onto the symbol  $x_k$  at the  $i$ th bit location. Note that,  $x_k$  is denoted as  $x_s$  for some  $s$  in space time code  $C = G_{STN}(x_1, x_2, \dots, x_S)$ . Due to the separate decoding property of STBC, the decision metric for  $x_k$  can be written as

$$|y_k - x|^2 + \beta |x|^2. \quad (8)$$

where  $y_k$  is equal to  $y$  of (4). Then, using (1) and (8), the ML soft decision bit metric for the bit  $c_{k'}$  can be written as

$$\begin{aligned} \lambda^i(c_{k'}) &= \min_{x \in \chi_{c_{k'}}^i} |y_k - x|^2 + \beta |x|^2 \\ &= \min_{x \in \chi_{c_{k'}}^i} [\Re(y_k) - \Re(x)]^2 + [\Im(y_k) - \Im(x)]^2 + \\ &\quad \beta [\Re^2(x) + \Im^2(x)]. \end{aligned} \quad (9)$$

In order to find the bit metrics given in equation (9), one has to have the subsets  $\chi_b^i$ ;  $i = 0, 1, \dots, m-1$ ,  $b \in \{0, 1\}$  of the signal map  $\chi$ . Figures 2 (a)-(h) show the subsets of a 16 QAM signal map. Decision regions for the constellation points in the subsets are also shown. As can be seen on the figures, the decision regions are not right in the middle of the two adjacent constellation points. The new decision regions for 16 QAM are given by the lines  $2\kappa d$ ,  $-2\kappa d$ , where  $\kappa = \beta + 1$ , and  $2d$  is the minimum distance between two constellation points. Note that, the decision regions of the subsets for any  $M$ -ary QAM constellation can be found easily in the same manner. Therefore, it is straightforward to generalize the results to  $M$ -ary QAM case.

Let's define  $x_{c_{k'}}^i$  as the constellation point where the metric (9) is minimum  $\forall x \in \chi_{c_{k'}}^i$ , and assume that  $0 \leq i \leq m/2 - 1$ . Then, it is easy to see from the decision regions in Figures 2

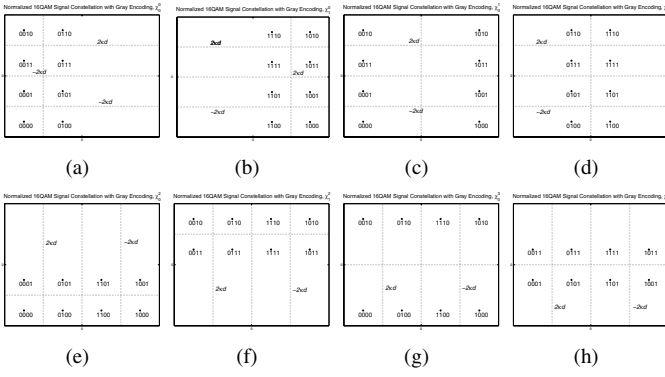


Fig. 2. Subsets of 16 QAM constellation with Gray labeling. Decision regions for BICM-STBC are shown with dotted lines. (a)  $\chi_0^0$ , (b)  $\chi_1^0$ , (c)  $\chi_0^1$ , (d)  $\chi_1^1$  (a)  $\chi_0^2$ , (b)  $\chi_1^2$ , (c)  $\chi_0^3$ , (d)  $\chi_1^3$

(a)-(d) that for a fixed  $i$ , the quadrature values of  $x_{c_{k'}=0}^i$  and  $x_{c_{k'}=1}^i$  are the same. Hence,  $[\Im(y_k) - \Im(x_{c_{k'}}^i)]^2$  is the same for  $c_{k'} = 0$  and  $c_{k'} = 1$ . Therefore for  $i = 0, 1, \dots, m/2 - 1$ , distance on the imaginary axis has no effect on making a decision about  $c_{k'}$  in (9). Similarly, for  $i = m/2, \dots, m - 1$   $[\Re(y_k) - \Re(x_{c_{k'}}^i)]^2$  is the same for  $c_{k'} = 0$  and  $c_{k'} = 1$  (see Figures 2 (e)-(h) for 16 QAM case), and therefore has no effect on making a decision about  $c_{k'}$  in (9). Consequently, the two-dimensional metric given in equation (9) reduces to an one-dimensional distance square.

$$\lambda^i(c_{k'}) = \begin{cases} \min_{\tilde{x} \in \tilde{\chi}_{c_{k'}}^i} [\Re(y_k) - \tilde{x}]^2 + \beta \tilde{x}^2, & i = 0, \dots, m/2 - 1 \\ \min_{\tilde{x} \in \tilde{\chi}_{c_{k'}}^i} [\Im(y_k) - \tilde{x}]^2 + \beta \tilde{x}^2, & i = m/2, \dots, m - 1 \end{cases} \quad (10)$$

where

- $\tilde{\chi}$ : set of constellation points on the real line  $\mathbb{R}^1$
- $\tilde{\chi}_b^i$ : subset of  $\tilde{\chi}$  where the  $i^{th}$  bit is equal to  $b \in \{0, 1\}$
- $i = 0, 1, \dots, m/2 - 1$
- $\tilde{i} = \begin{cases} i, & i = 0, 1, \dots, m/2 - 1 \\ i - m/2, & i = m/2, \dots, m - 1 \end{cases}$
- $\tilde{x}$ : elements of  $\tilde{\chi}$

#### A. Log-Likelihood Ratio (LLR) Bit Metrics

In this section we will provide simplified LLR bit metrics. These soft decision bit metrics are specifically formulated for  $M$ -ary QAM constellations labeled as in the IEEE 802.11a standard [14] (see Figure 3). As will be shown in Section V, even though these metrics are sub-optimal, they lead to the same results as the metrics of (10). Assuming equi-probability and using (10), the LLR of bit  $c_{k'} = 1$  (note that for  $c_{k'} = 0$ , the sign is reversed) can be written as

$$LLR(c_{k'}) = \log \frac{\max_{x \in \chi_1^i} P[y_k | x_k = x]}{\max_{x \in \chi_0^i} P[y_k | x_k = x]} \quad (11)$$

$$= \min_{\tilde{x} \in \tilde{\chi}_0^i} [\tilde{y}_k - \tilde{x}]^2 + \beta \tilde{x}^2 - \min_{\tilde{x} \in \tilde{\chi}_1^i} [\tilde{y}_k - \tilde{x}]^2 + \beta \tilde{x}^2 \quad (12)$$

$$= 2\tilde{y}_k(\tilde{x}_1 - \tilde{x}_0) - (\tilde{x}_1^2 - \tilde{x}_0^2)\kappa \quad (13)$$

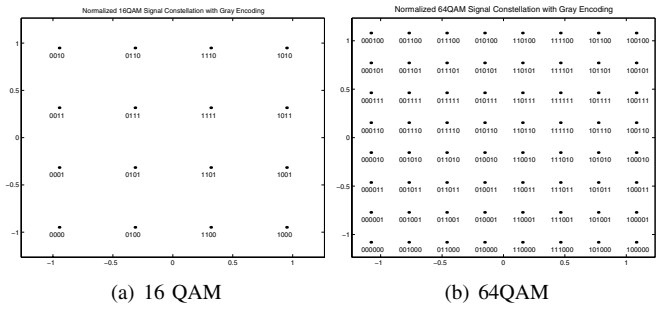


Fig. 3. Gray labeling used in 802.11a for (a) 16 QAM (b) 64 QAM

where  $\tilde{y}_k = \Re(y_k)$  or  $\Im(y_k)$  depending on the bit location  $i$ , and  $\tilde{x}_b \in \tilde{\chi}_b^i$  gives the minimum metric over the subconstellation  $\tilde{\chi}_b^i$ . Equation (12) follows from (11) using (1), (8) - (10). For the constellations of 802.11a/g (of Figure 3), once all the bit metrics are scaled down by their common factor  $4d$ , LLR bit metrics are given by, for 16 QAM,

$$\lambda^i(c_{k'}) = \begin{cases} \tilde{y}_k, & |\tilde{y}_k| \leq 2\kappa d & \tilde{i} = 0 \\ 2\tilde{y}_k - 2\kappa d, & \tilde{y}_k > 2\kappa d & \tilde{i} = 0 \\ 2\tilde{y}_k + 2\kappa d, & \tilde{y}_k < -2\kappa d & \tilde{i} = 0 \\ -|\tilde{y}_k| + 2\kappa d, & & \tilde{i} = 1 \end{cases} \quad (14)$$

and for 64 QAM,

$$\lambda^i(c_{k'}) = \begin{cases} \tilde{y}_k, & |\tilde{y}_k| \leq 2\kappa d & \tilde{i} = 0 \\ 2(\tilde{y}_k - \kappa d), & 2\kappa d < \tilde{y}_k \leq 4\kappa d & \tilde{i} = 0 \\ 3(\tilde{y}_k - 2\kappa d), & 4\kappa d < \tilde{y}_k \leq 6\kappa d & \tilde{i} = 0 \\ 4(\tilde{y}_k - 3\kappa d), & 6\kappa d < \tilde{y}_k & \tilde{i} = 0 \\ 2(\tilde{y}_k + \kappa d), & -4\kappa d < \tilde{y}_k \leq -2\kappa d & \tilde{i} = 0 \\ 3(\tilde{y}_k + 2\kappa d), & -6\kappa d < \tilde{y}_k \leq -4\kappa d & \tilde{i} = 0 \\ 4(\tilde{y}_k + 3\kappa d), & \tilde{y}_k < -6\kappa d & \tilde{i} = 0 \\ 2(-|\tilde{y}_k| + 3\kappa d), & |\tilde{y}_k| \leq 2\kappa d & \tilde{i} = 1 \\ -|\tilde{y}_k| + 4\kappa d, & 2\kappa d < |\tilde{y}_k| \leq 6\kappa d & \tilde{i} = 1 \\ 2(-|\tilde{y}_k| + 5\kappa d), & 6\kappa d < |\tilde{y}_k| & \tilde{i} = 1 \\ |\tilde{y}_k| - 2\kappa d, & |\tilde{y}_k| \leq 4\kappa d & \tilde{i} = 2 \\ -|\tilde{y}_k| + 6\kappa d, & 4\kappa d < |\tilde{y}_k| & \tilde{i} = 2 \end{cases} \quad (15)$$

The bit metrics of (14) and (15) can be further simplified to, for 16 QAM,

$$\lambda^i(c_{k'}) = \begin{cases} \tilde{y}_k, & \tilde{i} = 0 \\ -|\tilde{y}_k| + 2\kappa d, & \tilde{i} = 1 \end{cases} \quad (16)$$

and for 64 QAM,

$$\lambda^i(c_{k'}) = \begin{cases} \tilde{y}_k, & \tilde{i} = 0 \\ -|\tilde{y}_k| + 4\kappa d, & \tilde{i} = 1 \\ -|\tilde{y}_k| - 4\kappa d + 2\kappa d, & \tilde{i} = 2 \end{cases} \quad (17)$$

The decrease in the implementation complexity of the decoder, when the proposed new metrics are used, is illustrated in Table I. Note that, for the comparisons in the table the number of real calculations needed to find  $\beta$  and  $\kappa$  are excluded. Also, the number of calculations needed are given once  $y_k$ s are calculated for a fair comparison between all the bit metrics. As can be seen from the table that the new BICM-STBC bit metrics decrease the complexity of the decoder substantially.

TABLE I

THE NUMBER OF REAL MULTIPLICATIONS, ADDITIONS, SUBTRACTIONS, AND COMPARISONS USED FOR THE 2-D METRIC (9), THE 1-D METRIC (10), AND THE LLR BIT METRICS

$M$ -ary	Multiplications			Additions			Subtractions			Comparisons		
	2-D	1-D	LLR	2-D	1-D	LLR	2-D	1-D	LLR	2-D	1-D	LLR
4	10	3	0	6	1	0	4	1	0	2	1	0
16	40	6	1	24	2	0	16	2	0.5	8	2	0
64	160	12	2	96	4	0	64	4	1	32	4	0

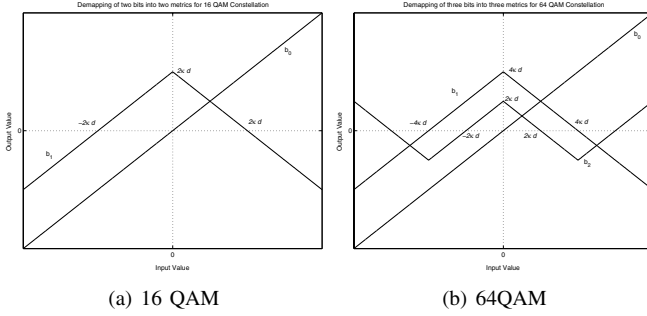


Fig. 4. (a) LLR bit metrics for 16 QAM (b) LLR bit metrics for 64 QAM

## V. RESULTS

We ran simulations on BICM-STBC-OFDM of [10], which was shown to achieve the maximum diversity in space and time. 64 states 1/2 rate *de facto* standard convolutional code is used to code the bits. The interleaver of 802.11a follows the encoder before the modulator. Each OFDM symbol has 64 subcarriers. The channel is modeled as frequency selective with equal power at each tap. The rms channel delay spread is 50 ns, and the maximum delay spread is 10 times the rms value. Figure 5 illustrates the results using different metrics for 16 and 64 QAM. It can be easily seen that the high complexity ML bit metrics of (9), low complexity ML bit metrics (10), and the LLR bit metrics of (14) and (15) achieve the same performance. Simulation results also show that quantizing the LLR bit metrics to 5 bits is sufficient. Simulation results of BICM-OFDM with 1 transmit and 1 receive antenna are presented for comparison.

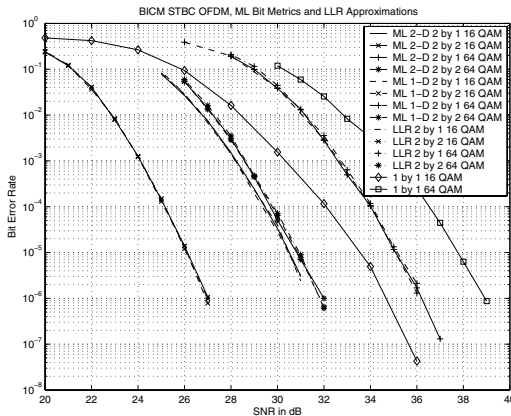


Fig. 5. BER vs SNR in dB curves for high and low complexity ML bit metrics and LLR bit metrics

## VI. CONCLUSION

It was shown earlier that combining BICM and STBC along with OFDM leads to a system that can achieve the maximum diversity in frequency and space. However, the decoding complexity of such a system appears to be significantly high. In this paper we showed that the bit metrics of a BICM-STBC system can be simplified from a distance calculation on the complex plane within  $M/2$  points to a distance calculation on the real line within  $\sqrt{M}/2$  points for  $M$ -ary QAM. This reduces the decoder complexity substantially while keeping the same high performance. Furthermore, we presented LLR approximations to ML bit metrics. The LLR bit metrics are specifically calculated for 16 and 64 QAM modulations given in wireless local area network standards IEEE 802.11a/g. Simulation results showed that the low complexity bit metrics achieve the same performance as their original high complexity counterparts.

## REFERENCES

- [1] E. Zehavi, "8-PSK trellis codes for a Rayleigh channel," *IEEE Trans. Commun.*, vol. 40, no. 5, pp. 873–884, May 1992.
- [2] G. Ungerboeck, "Channel coding with multilevel/phase signals," *IEEE Trans. Inform. Theory*, vol. IT-28, no. 1, pp. 55–67, January 1982.
- [3] G. Caire, G. Taricco, and E. Biglieri, "Bit-interleaved coded modulation," *IEEE Trans. Inform. Theory*, vol. 44, no. 3, May 1998.
- [4] V. Tarokh, N. Seshadri, and A. Calderbank, "Space-time codes for high data rate wireless communication: Performance criterion and code construction," *IEEE Trans. Inform. Theory*, vol. 44, no. 2, pp. 744–765, March 1998.
- [5] V. Tarokh, H. Jafarkhani, and A. Calderbank, "Space-time block codes from orthogonal designs," *IEEE Trans. Inform. Theory*, vol. 45, no. 5, pp. 1456–1467, July 1999.
- [6] —, "Space-time block coding for wireless communications: Performance results," *IEEE J. Select. Areas Commun.*, vol. 17, no. 3, pp. 451–460, March 1999.
- [7] H. Bolcskei and A. J. Paulraj, "Space-frequency coded broadband OFDM systems," in *Proc. WCNC*, vol. 1, September 2000, pp. 1–6.
- [8] B. Lu and X. Wang, "Space-time code design in OFDM systems," in *Proc. IEEE GLOBECOM*, vol. 2, 27 Nov - 1 Dec 2000, pp. 1000–1004.
- [9] E. Akay and E. Ayanoglu, "Full frequency diversity codes for single input single output systems," in *IEEE VTC Fall '04*, Los Angeles, USA, September 2004.
- [10] —, "Bit interleaved coded modulation with space time block codes for OFDM systems," in *IEEE VTC Fall '04*, Los Angeles, USA, September 2004.
- [11] —, "Low complexity decoding of bit interleaved coded modulation," in *Proc. IEEE ICC*, vol. 2, Paris, France, June 2004, pp. 901–905.
- [12] —, "High performance viterbi decoder for OFDM systems," in *Proc. IEEE VTC Spring*, Milan, Italy, May 2004.
- [13] F. Tosato and P. Bisaglia, "Simplified soft-output demapper for binary interleaved COFDM with application to HIPERLAN/2," in *Proc. IEEE ICC*, vol. 2, 2002, pp. 664–668.
- [14] IEEE 802.11a standard: Wireless LAN medium access control (MAC) and physical layer (PHY) specifications. High-speed physical layer in the 5 GHz band. IEEE. [Online]. Available: <http://standards.ieee.org/getieee802/802.11.html>